Technische Universität Graz

Adjoint sampling methods for electromagnetic scattering

H. Egger, M. Hanke, C. Schneider, J. Schöberl, S. Zaglmayr

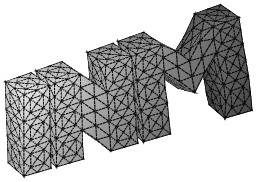

Berichte aus dem Institut für Numerische Mathematik

Bericht 2009/11

Technische Universität Graz

Adjoint sampling methods for electromagnetic scattering

H. Egger, M. Hanke, C. Schneider, J. Schöberl, S. Zaglmayr

Berichte aus dem Institut für Numerische Mathematik

Bericht 2009/11

Technische Universität Graz
Institut für Numerische Mathematik
Steyrergasse 30
A 8010 Graz

WWW: `http://www.numerik.math.tu-graz.at`

© Alle Rechte vorbehalten. Nachdruck nur mit Genehmigung des Autors.

ADJOINT BASED SAMPLING METHODS FOR ELECTROMAGNETIC SCATTERING

H. EGGER*, M. HANKE†, C. SCHNEIDER†, J. SCHÖBERL‡, AND S. ZAGLMAYR*

ABSTRACT. In this paper we investigate the efficient realization of sampling methods, based on solutions of certain adjoint problems. This adjoint approach does not require the explicit knowledge of a Green's function for the background medium, and allows to sample for all points and all dipole directions simultaneously; thus several limitations of standard sampling methods are relieved. A detailed derivation of the adjoint approach is presented for two electromagnetic model problems, but the framework can be applied to a much wider class of problems. We also discuss a relation of the adjoint sampling method to standard backprojection algorithms, and present numerical tests that illustrate the efficiency of the adjoint approach.

1. INTRODUCTION

Electromagnetic prospection deals with the determination of electric or magnetic inhomogeneities in a known background medium. Typical problems are the localization of conducting objects from scattered electromagnetic waves, or the reconstruction of conductivity or permittivity distributions inside a body from measurements of electro-static or -quasistatic fields. Such problems arise in many applications ranging from the detection of buried landmines or the identification of airplanes by radar, to medical imaging and nondestructive testing. For details and further applications, we refer to [6, 1].

In this paper, we consider two model problems, namely the scattering of time harmonic electromagnetic waves from perfectly conducting objects, and the effect of paramagnetic inclusions on magnetostatic fields. The corresponding inverse problems then consist of determining the areas of the inclusions from near field measurements of the electromagnetic fields. In principle, these nonlinear ill-posed problems can be solved by standard methods, like nonlinear Tikhonov regularization. However, such black-box approaches typically require heavy computations, and therefore linearizations or other approximations are frequently used in order to facilitate fast reconstructions. The resulting schemes then naturally suffer from these approximations, and therefore have a limited range of applicability.

An alternative class of methods, established over the past years for a variety of problems, are linear sampling and probe methods, cf., e.g., [18, 14, 22], and the references therein. These methods allow to test whether a point or a region belongs to a scattering object, without the need to iteratively solve forward problems for different parameter constellations. Therefore, sampling and probe methods enable

* Institute for Computational Mathematics, Graz University of Technology, Austria.
† Institute of Mathematics, Johannes Gutenberg University Mainz, Germany.
‡ Center for Computational Engineering Science, RWTH Aachen University, Germany.

rapid reconstructions, at least in principle. The methods we have in mind are based on range criteria of the following form

$$z \in D, \qquad \text{if and only if} \qquad g_{z,p} \in \mathcal{R}(L).$$

Here, the operator L stems from a factorization of the measurement operator [17, 10], and D denotes the support of the scatterer. The test functions $g_{z,p}$ are related to a fundamental solution or a Green's function for the underlying problem with singularity at a point z, and typically depend on an additional parameter (vector) p, which can be chosen in order to improve the results. The test, whether $g_{z,p}$ is in the range of the compact operator L, can be realized by Picard's criterion: If $\{\sigma_j, u_j, v_j\}$ denotes the singular system of L, then

$$g_{z,p} \in \mathcal{R}(L), \qquad \text{if and only if} \qquad \sum_j \sigma_j^{-2} |(g_{z,p}, v_j)|^2 < \infty.$$

The efficient implementation of a range test thus requires (i) a singular value decomposition of the operator L, which is directly related to the measurements and can be computed easily; (ii) the fast evaluation of the scalar products $(g_{z,p}, v_j)$, which requires the explicit knowledge of a fundamental solution for the problem under investigation. We would like to remark that other methods, e.g., the MUSIC algorithm [9, 16], or the linear sampling method [5], also rely on the knowledge and fast evaluation of Green's functions or fundamental solutions [7, 14].

In this paper, we present an alternative evaluation formula for the integrals $(g_{z,p}, v_j)$, which does not require an explicit representation of a Green's function. Related approaches based on *reciprocity gap functionals* have been investigated in connection with linear sampling methods [3, 4, 2]. The main result of our paper will be an identity of the form

$$(g_{z,p}, v_j) = p \cdot V_j(z), \tag{1}$$

where the functions V_j can be computed directly from the singular vectors v_j of the measurement operator. This formula does not require the knowledge of the Green's function; moreover, the dependence on the parameter p is made explicit, which allows to compute the range criterion easily for all parameter vectors p and test points z, as soon as the functions V_j have been computed. We will present this *adjoint* approach in detail for two electromagnetic model problems. The approach, however, is applicable to a much wider class of problems, e.g., electrical impedance or optical tomography.

The outline of this paper is as follows: In Section 2, we investigate the electromagnetic scattering from a perfect conductor. After introducing the relevant equations, we recall some details of the factorization method and the linear sampling method, and then derive an identity of the form (1). In Section 3, we consider a magnetostatic model problem, for which the factorization method provides somewhat stronger results, and again derive an identity of the form (1). In Section 4, we establish a connection between the factorization method and backprojection methods, i.e., we show that in some cases, the linear sampling method can be interpreted as a nonlinear backprojection algorithm. This implies that linear sampling and backprojection methods can easily be integrated into one algorithm, which

then provides additional quantitative information, that is usually missing in sampling methods. We conclude with presenting results of numerical experiments that illustrate the efficiency of the adjoint approach.

2. Electromagnetic scattering from a perfect conductor

The propagation of time harmonic electromagnetic fields generated by a current source $\mathcal{J}_S$ in a medium with constant permeability μ_0 is described by Maxwell's equations

$$\operatorname{curl}\mathcal{E} = \mathrm{i}\omega\mu_0\mathcal{H}, \qquad \operatorname{curl}\mathcal{H} = (\sigma - \mathrm{i}\omega\epsilon)\mathcal{E} + \mathcal{J}_S. \tag{2}$$

Here, $\mathcal{E}$ and $\mathcal{H}$ are the complex amplitudes of the electric and magnetic fields, respectively, the functions ϵ and σ denote the permittivity and conductivity distributions of the background medium, and ω is the angular frequency. If the current source $\mathcal{J}_S$ is locally supported, and the medium is homogeneous outside a sufficiently large ball (i.e., $\epsilon(x) = \epsilon_0$, $\sigma(x) = 0$ for $|x| \geq R'$), then the electromagnetic fields satisfy the Silver-Müller radiation condition

$$\lim_{|x|\to\infty} (\sqrt{\mu_0}\mathcal{H} \times x - |x|\sqrt{\epsilon_0}\mathcal{E}) = 0. \tag{3}$$

For a numerical realization, it is often advantageous to restrict the computational domain to a finite set, in which case the radiation condition has to be replaced by an appropriate boundary condition. Below we will only consider problems restricted to a large ball $\Omega = \{x \in \mathbb{R}^3 : |x| < R\}$ with $R > R'$, and we replace the radiation condition by an absorbing boundary condition [19, Section 1.2]

$$\nu \times \mathcal{H} + \sqrt{\epsilon_0/\mu_0}(\nu \times \mathcal{E}) \times \nu = 0 \qquad \text{on } \partial\Omega, \tag{4}$$

where ν denotes the outward pointing unit normal vector on $\partial\Omega$. Instead of this local boundary condition, one might as well consider nonlocal, exact boundary conditions based on Calderon maps [19, Section 9.4].

For the rest of this section, we shall further assume that the electric parameters ϵ and σ of the background medium are piecewise constant, i.e., we assume that $\epsilon = \epsilon'$ and $\sigma = \sigma'$ in some smooth domain $\Omega' \subset \Omega$, and $\epsilon = \epsilon_0$ and $\sigma = 0$ outside Ω'; here, ϵ', $\epsilon_0 > 0$, and $\sigma' \geq 0$ are known constants. This assumption simplifies our presentation, as we can refer to results from previous work. The main results presented in this paper however hold for more general material parameters. Finally, we assume that the source currents $\mathcal{J}_S$ are supported on a smooth open surface $S \subset \Omega \setminus \overline{\Omega'}$, and thus the material is homogeneous in the vicinity of S. For a sketch of the geometry, we refer to Figure 1 in Section 5.

2.1. Governing equations and basic notation.

Let the smooth domain $D \subset \Omega'$ be the support of a perfectly conducting inclusion. By the usual scaling $E = \sqrt{\epsilon_0}\mathcal{E}$, $J_S = \mathrm{i}\omega\mu_0\sqrt{\epsilon_0}\mathcal{J}_S$, and after elimination of the magnetic field $\mathcal{H}$, the scaled electric field can be seen to satisfy

$$\operatorname{curl}\operatorname{curl} E - k^2 n(x) E = J_S \qquad \text{in } \Omega \setminus \overline{D}, \tag{5}$$

$$\nu \times E = 0 \qquad \text{on } \partial D, \tag{6}$$

where the (positive) wave number k is defined by $k^2 = \epsilon_0\mu_0\omega^2$, and the function $n(x) = \epsilon_0^{-1}[\mathrm{i}\sigma(x)/\omega + \epsilon(x)]$ denotes the refractive index of the background. According to our remarks above, the system (5)–(6) is complemented by the absorbing

boundary condition

$$\nu \times \operatorname{curl} E + \mathrm{i}k(\nu \times E) \times \nu = 0 \qquad \text{on } \partial\Omega \tag{7}$$

Note that the case $\Omega = \mathbb{R}^3$ can be considered similarly, if (7) is replaced by a radiation condition or a non-local boundary condition [19]. Unique solvability of the boundary value problem (5)–(7) follows with standard arguments, cf. [19, Section 4]. The following result also holds for the special case $D = \emptyset$.

Lemma 1. *For any $J_S \in TH^{-1/2}(\operatorname{div}, S) \cap TL^2(S)$, the problem (5)–(7) has a unique solution $E \in H(\operatorname{curl}, \Omega \setminus \overline{D})$ that depends continuously on the data J_S.*

Here, $TL^2(S) = \{v \in L^2(S) : \nu \cdot v = 0\}$ denotes the space of square integrable tangential vector fields, and $TH^{-1/2}(\operatorname{div}, S) := \{v \in TH^{-1/2}(S) : \operatorname{div}_S v \in H^{-1/2}(S)\}$ is the space of functions with well-defined surface divergence; $H(\operatorname{curl}, \Omega) = \{v \in L^2(\Omega) : \operatorname{curl} v \in L^2(\Omega)\}$ denotes the space of functions with square integrable curl. For functions $v \in H(\operatorname{curl}, \Omega)$ the trace of the tangential components $(\nu \times v) \times \nu$ belongs to $TH^{-1/2}(\operatorname{curl}, \partial\Omega)$, which is the dual space of $TH^{-1/2}(\operatorname{div}, \partial\Omega)$. For details regarding these function spaces we refer to [19].

2.2. **The scattering problem.** As usual we decompose the total field $E = E^i + E^s$, where the incident field E^i satisfies (5) with $D = \emptyset$ and (7). By linearity of the equations, the scattered field $E^s = E - E^i$ then solves the system

$$\operatorname{curl}\operatorname{curl} E^s - k^2 n(x) E^s = 0 \qquad \text{in } \Omega \setminus D, \tag{8}$$

$$\nu \times E^s = -\nu \times E^i \qquad \text{on } \partial D, \tag{9}$$

$$\nu \times \operatorname{curl} E^s + \mathrm{i}k(\nu \times E^s) \times \nu = 0 \qquad \text{on } \partial\Omega. \tag{10}$$

Existence and uniqueness of the solutions E and E^i follow directly from Lemma 1, and the result for E^s follows because $E^s = E - E^i$. Note that since n was assumed to be piecewise constant, the incident field E^i has analytic components in Ω' [6, Section 6], and consequently $\nu \times E^i|_{\partial D}$ is well-defined and smooth. With the same arguments, it follows that E^s has analytic components in $\Omega \setminus \overline{\Omega'}$, and the tangential trace $(\nu \times E^s|_S) \times \nu$ is a well-defined and smooth function in $TL^2(S)$. This allows to define the measurement operator

$$M : TH^{-1/2}(\operatorname{div}, S) \cap TL^2(S) \to TL^2(S), \qquad J_S \mapsto (\nu \times E^s|_S) \times \nu, \tag{11}$$

that assigns to any surface excitation current J_S the corresponding tangential component of $E^s|_S$ of the scattered electric field. The following properties of the measurement operator are direct consequences of the definition of the fields E^i and E^s.

Lemma 2. *The operator M can be extended to a compact linear operator from $TL^2(S)$ to $TL^2(S)$. Moreover, there holds the decomposition $M = LG$, where $G : TL^2(S) \to TH^{-1/2}(\operatorname{div}, \partial D)$ and $L : TH^{-1/2}(\operatorname{div}, \partial D) \to TL^2(S)$ are linear compact operators defined by $G : J_S \mapsto \nu \times E^i|_{\partial D}$, and $L : -\nu \times E^i|_{\partial D} \mapsto (\nu \times E^s|_S) \times \nu$.*

Proof. The result was proven in [12] for the magnetic field formulation and unbounded domains, but the methods of proof carry over verbatim to the case considered here. The proof relies on a-priori bounds for solutions E^i and E^s and the continuity of the tangential trace map. The compactness of the operator follows

from the regularity of the scattered field; since the medium is assumed to be piecewise homogeneous, we know (cf. [6, Section 6]) that E^s has analytic components in the vicinity of S, and thus $(\nu \times E^s|_S) \times \nu$ is a smooth function. The compactness then follows by compact embedding. □

2.3. **A linear sampling method.** Let $\mathbb{G}(x,z)$ denote the Green's tensor corresponding to the problem (5)–(7) with $D = \emptyset$, i.e., for any $p \in \mathbb{R}^3$ the function $G_{z,p} = \mathbb{G}(\cdot,z)p$ is a solution of

$$\operatorname{curl}\operatorname{curl} G_{z,p} - k^2 n(x) G_{z,p} = \delta_z p \qquad \text{in } \Omega, \tag{12}$$

$$\nu \times \operatorname{curl} G_{z,p} + \mathrm{i}k(\nu \times G_{z,p}) \times \nu = 0 \qquad \text{on } \partial\Omega, \tag{13}$$

in the sense of distributions. The first equation implies that for any sufficiently smooth E satisfying $\operatorname{curl}\operatorname{curl} E - k^2 n(x) E = 0$ in some ball $B_r(z) = \{x \in \mathbb{R}^3 : |x-z| < r\} \subset \Omega$ there holds

$$p \cdot \overline{E}(z) = (\nu \times \operatorname{curl} G_{z,p}, E)_{\partial B_r(z)} - (G_{z,p}, \nu \times \operatorname{curl} E)_{\partial B_r(z)}. \tag{14}$$

Here and below, $(u,v)_S = \int_S u \cdot \overline{v} ds$ denotes the L^2 scalar product of complex vector fields. Formula (14) follows directly from the definition of the Green's function and integration by parts, cf. [19, Thm. 3.31].

Remark 1. For $n \equiv 1$ in Ω, the representation (14) is just a consequence of the Stratton-Chu formula, cf. [19, Theorem 12.2]. In this case, the function $G_{z,p}$ can be constructed explicitly: Let

$$\Phi(x,z) = \frac{1}{4\pi} \frac{e^{\mathrm{i}k|x-z|}}{|x-z|}, \qquad x \neq z,$$

denote the fundamental solution of the Helmholtz equation, and

$$\widetilde{\mathbb{G}}(x,z) = \Phi(x,z)\mathbb{I} + k^{-2} \nabla_z \nabla_z \Phi(x,z)$$

be the dyadic Green's function for Maxwell's equations [19, Section 12]. Denote $\widetilde{G}_{z,p} = \widetilde{\mathbb{G}}(x,z)p$, then the solution $G_{z,p}$ of (12)–(13) is given by $G_{z,p} = \widetilde{G}_{z,p} + V_{z,p}$ where $V_{z,p}$ solves (8) in Ω with boundary conditions

$$\nu \times \operatorname{curl} V_{z,p} + \mathrm{i}k(\nu \times V_{z,p}) \times \nu = -\nu \times \operatorname{curl} \widetilde{G}_{z,p} - \mathrm{i}k(\nu \times \widetilde{G}_{z,p}) \times \nu$$

on $\partial\Omega$. This implies that $G_{z,p}$ satisfies the homogeneous boundary condition (13).

The following result has been derived in slightly different form in [12] for the magnetic field formulation; see also [13] for corresponding results for the electric field formulation.

Lemma 3. *Let us define the test function $g_{z,p} := (\nu \times G_{z,p}|_S) \times \nu$. Then a point z belongs to D, if and only if, $g_{z,p} \in \mathcal{R}(L)$, with L as defined in Lemma 2.*

Proof. The proof is similar to the one in [13]; the boundary condition (13) is used to take care of the bounded domain. □

Together with the factorization stated in Lemma 2, we obtain the following (weak) characterization of the inclusion.

Corollary 1. *Let $p \neq 0$. If $g_{z,p} \in \mathcal{R}(M)$, then $z \in D$.*

Since the operator M is compact, it has a singular value decomposition, and the range criterion is equivalent to the Picard criterion. This yields the following formulation of the range test, which can efficiently be used in numerical computations.

Corollary 2. *Let $\{\sigma_j, u_j, v_j\}$ denote a singular system of M and $p \neq 0$. Then the condition $\sum_j \sigma_j^{-2} |(g_{z,p}, v_j)_S|^2 < \infty$ implies $z \in D$.*

Remark 2. The arguments used in Lemma 2 and Corollaries 1 and 2 hold for more general inhomogeneous background media. However, the numerical realization of a sampling method based on Corollary 2 requires the knowledge of a Green's function, or at least a fundamental solution of the underlying problem. Note that other sampling methods typically require the knowledge of fundamental solutions as well, cf. [7]. In effect, this restricts the applicability of many sampling methods to the case of homogeneous or sufficiently simple background media.

2.4. **An adjoint method.** The sampling method discussed in the previous section relies on the efficient computation of the integrals $(g_{z,p}, v_j)_S$. In practice, this evaluation has to be carried out for many points z and possibly several dipole directions p. In the following, we present a method that allows to compute these integrals without the use of an explicit representation of the Green's function.

For a given $v_j \in TH^{-1/2}(\mathrm{div}, S) \cap TL^2(S)$, let V_j be the solution of the adjoint problem

$$\mathrm{curl}\,\mathrm{curl}\, V_j - k^2 \overline{n}(x) V_j = v_j \qquad \text{in } \Omega \tag{15}$$

$$\nu \times \mathrm{curl}\, V_j - \mathrm{i}k(\nu \times V_j) \times \nu = 0 \qquad \text{on } \partial\Omega. \tag{16}$$

Existence and uniqueness of a solution $V_j \in H(\mathrm{curl}, \Omega)$ of (15)–(16) is again provided by Lemma 1. The following identity then follows readily by utilizing the definitions of the Green's function and the solution of the adjoint problem.

Theorem 1. *Let $g_{z,p}$ be defined as above. Then for any $v_j \in TH^{-1/2}(\mathrm{div}, S) \cap TL^2(S)$ and $z \in \Omega \setminus S$ there holds*

$$(g_{z,p}, v_j)_S = p \cdot \overline{V_j}(z),$$

where V_j denotes the solution of (15)–(16).

Proof. Let $B_r(z) = \{x \in \Omega : |x - z| \leq r\}$ be the ball around z with sufficiently small radius $r > 0$, and denote the outer normal of $B_r(z)$ by ν again. Using (15)–(16) and $g_{z,p} = (\nu \times G_{z,p}|_S) \times \nu$, we find that

$$\begin{aligned}(g_{z,p}, v_j)_S &= (\mathrm{curl}\, G_{z,p}, \mathrm{curl}\, V_j)_{\Omega \setminus B_r(z)} - (G_{z,p}, k^2 \overline{n}(x) V_j)_{\Omega \setminus B_r(z)} \\ &\quad - (G_{z,p}, \nu \times \mathrm{curl}\, V_j)_{\partial B_r(z)} + (G_{z,p}, \mathrm{i}k(\nu \times V_j) \times \nu)_{\partial\Omega} \\ &= -(G_{z,p}, \nu \times \mathrm{curl}\, V_j)_{\partial B_r(z)} + (\nu \times \mathrm{curl}\, G_{z,p}, V_j)_{\partial B_r(z)} = p \cdot \overline{V_j}(z),\end{aligned}$$

where the last equality follows from the Stratton-Chu formula (14). □

The alternative representation of the integrals provides the basis for a formulation of the sampling method without reference to the Green's function.

Corollary 3. *Let $\{\sigma_j, u_j, v_j\}$ denote a singular system of M, and let V_j be defined by* (15)–(16). *Then $g_{z,p} \in \mathcal{R}(M)$, if and only if, $\sum_j \sigma_j^{-2} |p \cdot V_j(z)|^2 < \infty$.*

Let us emphasize that this alternative formulation enables us to realize the range test for all points in the computational domain at once, as soon as the solutions V_j to the adjoint problems have been computed. Moreover, because of the explicit dependence on the direction p, we can easily compute the integrals $(g_{z,p}, v_j)_S$ for several directions.

Corollary 4. *Let $g_{z,p}$ and V_j be defined as above. Then*

$$\int_{|p|=1} |(g_{z,p}, v_j)_S|^2 dp = \frac{4\pi}{3} |V_j(z)|^2.$$

Remark 3. The statement of Corollary 3 does not change, if the terms $|p \cdot V_j(z)|$ are replaced by $|V_j(z)|$. Note, however, that for the electromagnetic scattering problem, the sampling method of Corollary 1, respectively its equivalent formulation of Corollary 3, allow only to characterize a subset $D' \subset D$ of the inclusion. Thus the use of several dipole directions p and the separate evaluation of the range criterion for different directions may increase the area of D', and thus provide a better estimate of the scatterer.

3. A scattering problem in magnetostatics

Let us now turn to a second model problem, for which the factorization method provides a sharper characterization of the domain occupied by the inclusion. Since the magnetic field is now static, all function spaces and inner products will be real in the following.

3.1. Problem formulation.

For $\omega = 0$, Maxwell's equations describing the magnetic field in a linear medium with inhomogeneous permeability μ read

$$\operatorname{curl} \mathcal{H} = \mathcal{J}_S, \qquad \operatorname{div}(\mu \mathcal{H}) = 0.$$

The second equation allows to represent the magnetic induction $\mu\mathcal{H}$ by a vector potential, which we denote by $\mathcal{E}$ again, i.e., $\mu\mathcal{H} = \operatorname{curl} \mathcal{E}$. Since adding a gradient field $\nabla\phi$ to the vector potential does not change the magnetic field $\mathcal{H}$, one can require $\mathcal{E}$ to satisfy additional *gauging* conditions. In the following, we utilize a Coulomb gauge, which forces $\mathcal{E}$ to be orthogonal to gradient fields, i.e., $\mathcal{E}$ has to be weakly divergence free. As a consequence of the first equation, $\mathcal{J}_S$ has to be (weakly) divergence free as well. After rescaling $E = \mu_0^{-1}\mathcal{E}$ and by rewriting $J_S = \mathcal{J}_S$, we obtain

$$\operatorname{curl} \gamma_r \operatorname{curl} E = J_S, \qquad \operatorname{div} E = 0 \qquad \text{in } \Omega, \tag{17}$$

where γ_r denotes the relative reluctivity defined by $\gamma_r = \mu_0/\mu$. As in the previous section, let Ω be a sufficiently large ball, and assume that γ_r is constant near $\partial\Omega$. We then complement (17) by homogeneous boundary conditions

$$\nu \times \operatorname{curl} E = 0, \qquad \nu \cdot E = 0 \qquad \text{on } \partial\Omega. \tag{18}$$

For ease of presentation we assume in the following that the background medium has constant reluctivity, i.e., $\gamma_r \equiv \gamma_0$ in $\Omega \setminus D$ for some constant γ_0. Moreover, we assume that the paramagnetic inclusion has a strictly smaller constant reluctivity, i.e., $\gamma_r \equiv \gamma_1$ in D with $0 < \gamma_1 < \gamma_0$. As in the previous section, we suppose that the excitation current J_S is supported on a smooth surface $S \subset \Omega \setminus \overline{D}$; for a sketch of the geometry see again Figure 1 in Section 5.

The unique solvability of the equations describing the magnetostatic vector potential follows from standard arguments, cf. [8, Chapter IX].

Lemma 4. *For any divergence free surface current $J_S \in TL^2_0(S) = \{v \in TL^2(S) : \int_S v \cdot \nabla\phi \, ds = 0 \quad \text{for all } \phi \in C^\infty(\Omega)\}$, problem (17)–(18) has a unique solution $E \in H(\operatorname{curl}, \Omega)$ depending continuously on J_S.*

The total field $E = E^i + E^s$ can again be decomposed into an incident field E^i that solves (17)–(18) with γ_r replaced by γ_0, and a scattered field E^s, which is due to the inhomogeneity, and satisfies

$$\operatorname{curl}\gamma_r \operatorname{curl} E^s = \operatorname{curl}(\gamma_0 - \gamma_r)\operatorname{curl} E^i, \qquad \operatorname{div} E^s = 0 \qquad \text{in } \Omega \tag{19}$$

$$\nu \times \operatorname{curl} E^s = 0, \qquad \nu \cdot E^s = 0 \qquad \text{on } \partial\Omega. \tag{20}$$

Unique solvability of this problem follows from Lemma 4 applied to E and E^i and the representation $E^s = E - E^i$. Note that for $\gamma_r = \gamma_0$, the scattered field vanishes.

3.2. **The measurement operator and the associated factorization method.** In the following, we define a measurement operator, which associates to any divergence free current J_S the corresponding trace of the tangential components of the scattered field.

Remark 4. For the results below, we have to factor out tangential traces of gradient fields, i.e., functions in $N(S) = \text{closure}\{(\nu \times \nabla\phi|_S) \times \nu : \phi \in C^\infty(\Omega)\}$, where the closure is taken with respect to $TL^2(S)$. We thus consider any $v \in TL^2(S)$ as representant of the equivalence class $v + N(S)$ in the factor space $TL^2(S)/N(S)$. This space can be identified with the dual space $TL^2_0(S)'$ of the space of divergence free tangential fields. For details, we refer to [11, 13].

Lemma 5. *Let us define the current-to-measurement map*

$$\widetilde{M} : TL^2_0(S) \to TL^2_0(S)', \qquad J_S \mapsto (\nu \times E^s|_S) \times \nu,$$

and let $\iota : TL^2_0(S) \to TL^2_0(S)'$ denote the Riesz isomorphism from $TL^2_0(S)$ into its dual. Then the measurement operator $M := \iota^{-1}\widetilde{M}$ is a compact, selfadjoint linear operator on $TL^2_0(S)$.

Proof. Apart from the self-adjointness, the result was proven in [13] for the operator $\iota M \iota^{-1} = \widetilde{M}\iota^{-1}$ in case of an unbounded domain. The methods of proof, however, also apply for the situation considered here. To see that M is selfadjoint, let J_1, $J_2 \in TL^2_0(S)$, and observe that

$$(\widetilde{M}J_1, J_2)_S = (\gamma_r \operatorname{curl} E_1^s, \operatorname{curl} E_2^s)_\Omega = (J_1, \widetilde{M}J_2)_S,$$

which then implies the self-adjointness of M. □

Remark 5. The restriction of the measurements $(\nu \times E^s|_S) \times \nu$ to the factor space $TL^2_0(S)'$, and the subsequent identification of this space with $TL^2_0(S)$ via the Riesz isomorphism amounts to a projection of the measurements onto the divergence free subspace $TL^2_0(S)$. Details concerning this projection are given in the next section.

For a characterization of the domain occupied by the inclusion, we utilize functions related to the Green's tensor for the magnetostatic equation. Here we define $G_{z,p}$ as solution of the problem

$$\operatorname{curl}\gamma_0 \operatorname{curl} G_{z,p} = \operatorname{curl}(\delta_z p), \qquad \operatorname{div} G_{z,p} = 0 \qquad \text{in } \Omega \tag{21}$$

$$\nu \times \operatorname{curl} G_{z,p} = 0, \qquad \nu \cdot G_{z,p} = 0 \qquad \text{on } \partial\Omega \tag{22}$$

in the sense of distributions.

Remark 6. For the case of a homogeneous background medium, e.g., $\gamma_0 \equiv 1$, the Green's function $G_{z,p}$ can be constructed explicitly. Let us define

$$\widetilde{G}_{z,p}(x) = \frac{1}{4\pi} \operatorname{curl} \frac{p}{|x-z|},$$

and let $V_{z,p}$ solve (17) with $J_S = 0$ and boundary conditions

$$\nu \times \operatorname{curl} V_{z,p} = -\nu \times \operatorname{curl} \widetilde{G}_{z,p}, \qquad \nu \cdot V_{z,p} = -\nu \cdot \widetilde{G}_{z,p} \qquad \text{on } \partial\Omega.$$

Then $G_{z,p} = \widetilde{G}_{z,p} + V_{z,p}$ satisfies (21)–(22). The arguments below are, however, also valid for more general background media.

The following result, which is the core of the factorization method considered here, has been proven in [13] for the case of unbounded domains. The corresponding result for bounded domains follows with the same arguments.

Lemma 6. *For some $p \in \mathbb{R}^3$, let us define the test function $g_{z,p} := (\nu \times G_{z,p}|_S) \times \nu$. Then $\iota^{-1} g_{z,p} \in \mathcal{R}(|M|^{1/2})$, if and only if $z \in D$.*

The compactness of the measurement operator and the Picard criterion yield the following range test, which can efficiently be used in computations.

Corollary 5. *Let $\{\lambda_j, v_j\}$ denote an eigensystem of M, and let $g_{z,p}$ be defined as above. Then $z \in D$, if and only if $\sum_j |\lambda_j|^{-1} |(g_{z,p}, v_j)_S|^2 < \infty$.*

Proof. Since $v_j \in TL_0^2(S)$, we have $(g_{z,p}, v_j)_S = (\iota^{-1} g_{z,p}, v_j)_S$, where we identified the function $g_{z,p}$ with the corresponding distribution. The result then follows from Lemma 6. □

An application of Corollary 5 requires the efficient evaluation of the inner products $(g_{z,p}, v_j)_S$, which in turn rely on the availability of an explicit representation of the Green's function, or, at least, a fundamental solution for the problem under investigation. Like for the electromagnetic scattering problem considered in the previous section, one can compute these integrals without knowledge of the Green's function, by utilizing solutions to certain adjoint problems.

3.3. **Adjoint formulation.** Let us consider the following adjoint problem, where v_j is a divergence free tangential current source.

$$\operatorname{curl} \gamma_0 \operatorname{curl} V_j = v_j, \qquad \operatorname{div} V_j = 0, \qquad \text{in } \Omega \tag{23}$$

$$\nu \times \operatorname{curl} V_j = 0, \qquad \nu \cdot V_j = 0 \qquad \text{on } \partial\Omega. \tag{24}$$

The unique solvability of this problem for any $v_j \in TL_0^2(S)$ follows from Lemma 4. For the solutions V_j of this adjoint problem, the following identities can be derived.

Theorem 2. *For given $v_j \in TL_0^2(S)$, let V_j denote the solution of (23)–(24). Then for every $p \in \mathbb{R}^3$ we have*

$$(g_{z,p}, v_j)_S = p \cdot \operatorname{curl} V_j(z),$$

where $g_{z,p}$ was defined as above. Moreover, there holds the identity

$$\int_{|p|=1} |(g_{z,p}, v_j)_S|^2 dp = \frac{4\pi}{3} |\operatorname{curl} V_j(z)|^2.$$

Proof. By the definition of V_j and $g_{z,p}$, we obtain

$$\begin{aligned}(g_{z,p}, v_j)_S &= -(\gamma_0 G_{z,p}, \nu \times \operatorname{curl} V_j)_{\partial B_r(z)} + (\gamma_0 \nu \times \operatorname{curl} G_{z,p}, V_j)_{\partial B_r(z)} \\ &= p \cdot \operatorname{curl} V_j(z),\end{aligned}$$

where the last equality follows from the definition of $G_{z,p}$ and integration by parts as in (14). The second identity then follows from integration over the unit sphere. □

As a direct consequence of this result, we obtain the following equivalent formulation of the range test, which does not rely on an explicit representation of the Green's function.

Corollary 6. *Let $\{\lambda_j, v_j\}$ denote an eigensystem of the measurement operator M, and let V_j be defined by (23)–(24). Then a point z belongs to the inclusion D, if and only if $\sum_j |\lambda_j|^{-1} |\operatorname{curl} V_j(z)|^2 < \infty$.*

Remark 7. The results of this section can be generalized to non-homogeneous background. However, we feel that already for the case of a homogeneous background, the alternative range test of Corollary 6 has many advantages, as it allows to sample efficiently for all points z and all directions p, as soon as the solutions V_j to the adjoint problems are available.

4. A connection to linear backprojection

In this section, we would like to highlight a connection of the adjoint formulation of the sampling method discussed in the previous section to linear backprojection, which can be considered to be a first step of nonlinear Landweber iteration or other iterative regularization methods, cf., e.g., [15].

4.1. Forward operators.

Let us consider the magnetostatic scattering problem with constant background medium, i.e., $\gamma_r \equiv \gamma_0$ in $\Omega \setminus \overline{D}$, and strictly smaller reluctivity $\gamma_r \equiv \gamma_1$ in D, as discussed in the previous section. Recall that the scattered field $E_J^s(\gamma_r)$ corresponding to a source J and the relative reluctivity distribution γ_r satisfies

$$\begin{aligned}\operatorname{curl} \gamma_r \operatorname{curl} E_J^s = \operatorname{curl}(\gamma_0 - \gamma_r) \operatorname{curl} E_J^i, \qquad & \operatorname{div} E_J^s = 0 \qquad && \text{in } \Omega, \\ \nu \times \operatorname{curl} E_J^s = 0, \qquad & \nu \cdot E_J^s = 0 \qquad && \text{in } \partial\Omega,\end{aligned}$$

where the incident field E_J^i is given by

$$\operatorname{curl} \gamma_0 \operatorname{curl} E_J^i = J, \qquad \operatorname{div} E_J^i = 0 \qquad \text{in } \Omega \tag{25}$$

$$\nu \times \operatorname{curl} E_J^i = 0, \qquad \nu \cdot E_J^i = 0 \qquad \text{in } \partial\Omega. \tag{26}$$

We define a nonlinear operator $\widetilde{F}_J : \mathcal{D}(F) \to TL_0^2(S)'$ that maps the reluctivity distribution to the (equivalence class of) measurements $(\nu \times E_J^s|_S) \times \nu$ of the scattered field corresponding to a specific source current J. Like in Lemma 5, we then define the forward operator $F_J := \iota^{-1} \widetilde{F}_J$, where $\iota : TL_0^2(S) \to TL_0^2(S)'$ is the Riesz isomorphism.

Remark 8. For $u \in TL^2(S)$, we define the restriction $\Pi : u \mapsto u - \nabla_S \phi$, where ∇_S denotes the surface gradient, and $\phi \in H^1(S)$ solves the variational problem

$$(\nabla_S \phi, \nabla_S \psi)_S = (u, \nabla_S \psi)_S \qquad \text{for all } \psi \in C^\infty(\Omega).$$

It follows that $\Pi u \in TL^2_0(S)$ for any $u \in TL^2_0(S)$; see also Remark 5. We then have $F_J(\gamma) = \Pi\big((\nu \times E^s_j|_S) \times \nu\big)$, and obtain $F_J(\gamma) = MJ$, where M is the measurement operator defined in Lemma 5.

The derivative of the forward operator F at γ_0 in direction h is given by $F'_J(\gamma_0)h = \Pi\big((\nu \times W^s_J|_S) \times \nu\big)$, where W^s_J is the solution of

$$\operatorname{curl} \gamma_0 \operatorname{curl} W^s_J = -\operatorname{curl} h \operatorname{curl} E^i_J, \qquad \operatorname{div} W^s_J = 0 \qquad \text{in } \Omega, \tag{27}$$

$$\nu \times \operatorname{curl} W^s_J = 0, \qquad \nu \cdot W^s_J = 0 \qquad \text{in } \partial\Omega. \tag{28}$$

The action of the adjoint of the derivative operator on some element $r \in TL^2_0(S)$ is then given by

$$\begin{aligned}(F'_J(\gamma_0)^* r, h)_{L^2(\Omega)} &= (r, F'_J(\gamma_0)h)_{TL^2(S)} = (r, (\nu \times W^s_J) \times \nu)_{TL^2(S)} \\ &= (\gamma_0 \operatorname{curl} E^i_r, \operatorname{curl} W^s_J)_{L^2(\Omega)} = -(h \operatorname{curl} E^i_r, \operatorname{curl} E^i_J)_{L^2(\Omega)},\end{aligned}$$

where E^i_r is the solution of (25)–(26) with J replaced by r, and the adjoint was taken with respect to the scalar products of $L^2(\Omega)$ and $TL^2(S)$. For $r \in TL^2_0(S)$, this yields the representation

$$F'_J(\gamma_0)^* r = -\operatorname{curl} E^i_r \cdot \operatorname{curl} E^i_J.$$

4.2. **Multiple excitations.** As a next step, we generalize these definitions to the case of multiple excitations: Let $M = M(\gamma_r)$ denote the measurement operator defined above corresponding to a reluctivity distribution γ_r. We then define the full forward operator $F : \gamma_r \to M(\gamma_r)$ by $F(\gamma_r)J := F_J(\gamma_r)$ for all $J \in TL^2_0(S)$.

The measurement space $\mathcal{L}(TL^2_0(S), TL^2_0(S))$ can be equipped with the Hilbert Schmidt norm defined by $|||A||| = \sqrt{((A,A))}$, where

$$((A,B)) = \sum_{i,j} (Av_j, Bv_i)_{TL^2(S)},$$

and $\{\lambda_j, v_j\}$ denotes an eigensystem of $M(\gamma_r)$. The action of the adjoint operator $F'(\gamma_0)^*$ on some element R in the measurement space is then defined by

$$\begin{aligned}(F'(\gamma_0)^* R, h)_{L^2(\Omega)} &= ((R, F'(\gamma_0)h)) = \sum_{i,j} (Rv_j, (\nu \times W_{v_i}|_S) \times \nu)_{TL^2(S)} \\ &= -\sum_{i,j} (h \operatorname{curl} U_j, \operatorname{curl} V_i)_{L^2(\Omega)},\end{aligned}$$

where W_{v_i} is defined by (27)–(28) with J replaced by v_i, and the functions U_j and V_i solve (25)–(26) with $J = Rv_j$ and $J = v_i$, respectively. Thus the action of the adjoint derivative is given by

$$F'(\gamma_0)^* R = -\sum_{i,j} \operatorname{curl} U_j \cdot \operatorname{curl} V_i. \tag{29}$$

4.3. **Linearization and backprojection.** For solving the nonlinear inverse problem $F(\gamma_r) = M$, we consider a formal linearization of the forward operator

$$F(\gamma_r) = F(\gamma_0) + F'(\gamma_0)(\gamma_r - \gamma_0) + o(||\gamma_r - \gamma_0||),$$

and we consider the linearized problem $F'(\gamma_0)(\gamma_r - \gamma_0) = M$ (note that $F(\gamma_0) = 0$) instead of the nonlinear problem. Applying a simple linear backprojection yields as a first approximation

$$\gamma_r \sim \gamma_0 + F'(\gamma_0)^* M,$$

thus we have to apply the adjoint of the derivative operator only to the special element $R = M$. Utilizing the fact, that v_j are the eigenvectors of M, we obtain $Rv_j = Mv_j = \lambda_j v_j$, and thus $U_j = \lambda_j V_j$. Inserting this into (29), we obtain the representation

$$F'(\gamma_0)^* M = -\sum_{i,j} \lambda_j \operatorname{curl} V_j \cdot \operatorname{curl} V_i \tag{30}$$

for the update of the linear backprojection method.

Remark 9. Note that the functions V_j are just the solutions of the adjoint problems (23)–(24), which were already used for the adjoint implementation of the factorization method. By replacing $\lambda_j \operatorname{curl} V_j$ in (30) by $-\delta_{ij}|\lambda_j|^{-1} \operatorname{curl} V_j$, we recover the sampling method of Corollary 6. In any case, the functions V_j that are required for the implementation of the range test of the sampling method can be re-used for the application of the backprojection, hence both methods can be implemented easily within one algorithm.

5. Numerical tests

Let us discuss the implementation of the adjoint sampling method for the scattering from a perfect conductor investigated in Section 2. For our numerical tests, we use the following geometry: $\Omega = B_5(0)$ is the ball around the origin with radius 5. For the refractive index of the background medium, we choose $n(x) = n' = 2 + \mathrm{i}$ in $\Omega' = B_1(0)$ and $n(x) \equiv 1$ in $\Omega \setminus \Omega'$, and the wavenumber is set to $k = 1$. The scatterer D is contained in the cube $[-0.5, 0.5]^2 \times [0.3, 0.5] \subset \Omega'$, as depicted in Figure 1. Finally, the excitations and measurements are located at the surface $S = \partial B_{1.1}(0) \cap \{z \geq 0\}$.

5.1. **Discretization by finite elements.** For the discretization of the electric field equations, we use an $H(\mathrm{curl})$-conforming finite element method with high order Nedelec finite elements [21, 24] consisting of piecewise polynomials with maximal degree 5. The space $TL^2(S)$ of excitation currents and measurements is approximated by the lowest order Nedelec space [20] restricted to the surface S. The measurement matrix then corresponds to a projection of the measurement operator (11) onto this finite element trace space, i.e., one source/detector is associated with each edge of the mesh on the measurement surface S. In our numerical test example, the total number of degrees of freedom of a finite element solution is $nd = 202.570$ and the number of independent sources/detectors is $ns = 171$. All computations were implemented in the open-source finite element software NETGEN/NgSolve [23].

A discretization of the problems (5)–(7) yields linear systems of the form

$$A(D)E_j = J_j, \qquad j = 1, \ldots, ns, \tag{31}$$

where $A(D)$ refers to the system matrix in the presence of a perfectly conducting scatterer located in D, and ns denotes the number of source (and detector) locations. The scattered fields defined by (8)–(10) with excitations J_i are then given by $E_j^s = E_j - E_j^i$, and the entries of the measurement matrix are obtained by evaluation of the tangential traces of E_j^s at the measurement surface.

Since the problems (31) have to be solved many times for different right hand sides, we utilized a sparse factorization of the $nd \times nd$ dimensional matrix $A(D)$;

the solutions of the systems (31) can then be computed very fast. The required computation times for this calibration procedure are listed in Table 1.

TABLE 1. Computation times for the sparse factorizations of the system matrices $A(D)$ using PARDISO [25], and the solution of (31) for 171 right hand sides. All computations were performed on a standard dual-core desktop PC.

assembling	factorization	solution	total
21s	416s	148s	585s

5.2. **Adjoint sampling method.** After computing a singular value decomposition $\{\sigma_j, u_j, v_j\}$ of the $ns \times ns$ dimensional measurement matrix, we have to determine the adjoint solutions V_j of (15)–(16), which are defined by linear systems of the form

$$A(\emptyset)\overline{V_j} = \overline{v_j}, \qquad j = 1, \ldots, ns.$$

Since the singular vectors $v_j = \sum_i v_{jk} J_k$ can be expressed via the sources J_k, we obtain $V_j = \sum_i v_{jk} \overline{E_k^i}$, where E_k^i denotes the solution of the forward problem without scatterer and current source J_k. Thus no further pde problems have to be solved here to find the adjoint solutions V_j. Even with real data, only the ns pde problems for determining E_k^i, $k = 1, \ldots, ns$ have to be solved, which can be done independently of the data in an initialization step.

For a quantitative evaluation of the range criterion of Corollary 3, we use the following numerical range test: For z on a uniform grid and some $0 < n \leq ns$, we compute

$$s_n(z) = C(z)^{-1} \sum_{j=1}^{n} \sigma_j^{-2} |V_j(z)|^2,$$

where the factors $C(z) := \left(\sum_{j=1}^{ns} |V_j(z)|^2 \right) = \frac{4\pi}{3} \int_{S^2} \|g_{z,p}\|_S^2 dp$ are intended to facilitate a comparison of the resulting numbers for different sampling points with each other. In our numerical example, we chose the truncation index n by $\sigma_{n+1} < \delta\sigma_1 \leq \sigma_n$ with $\delta = 10^{-6}$, which in this case amounts to $n = 96$. In general, the truncation level δ will depend on the noise of the data. Alternatively, one could replace the denominator σ_j^2 by $\sigma_j^2 + \alpha$ for some $\alpha > 0$ and set $n = ns$; cf. [14] for different implementations of numerical range tests. The isolines and isosurfaces of the function $c_n(z) = \log(s_n(z))$ are displayed in Figure 1.

5.3. **Discrete identity.** At the end of this section, we would like to make a remark concerning the adjoint approach on the discrete level. The identities of Theorem 1 and 2 also hold for discretizations in the following sense: Let $V_h \subset H(\mathrm{curl}, \Omega)$ denote a conforming finite element space, and let $G_{z,p}^h$ denote the discrete Green's function corresponding to (12)–(13), i.e., $G_{z,p}^h \in V_h$ such that

$$(\mathrm{curl}\, G_{z,p}^h, \mathrm{curl}\, v_h)_\Omega - k^2 (n(x)\, G_{z,p}^h, v_h)_\Omega + ik (G_{z,p}^h, (\nu \times v_h) \times \nu)_{\partial\Omega} = p \cdot \overline{v}_h(z)$$

for all $v_h \in V_h$. Since the test functions v_h are in general not continuous on Ω, the evaluation points z have to be restricted to the interior of the individual elements. Accordingly, we define V_j^h as the solutions of the discrete adjoint problems

$$(V_j^h, v_h)_\Omega - k^2 (\overline{n}(x)\, V_j^h, v_h)_\Omega - ik (V_j^h, (\nu \times v_h) \times \nu)_{\partial\Omega} = (v_j, v_h)_S$$

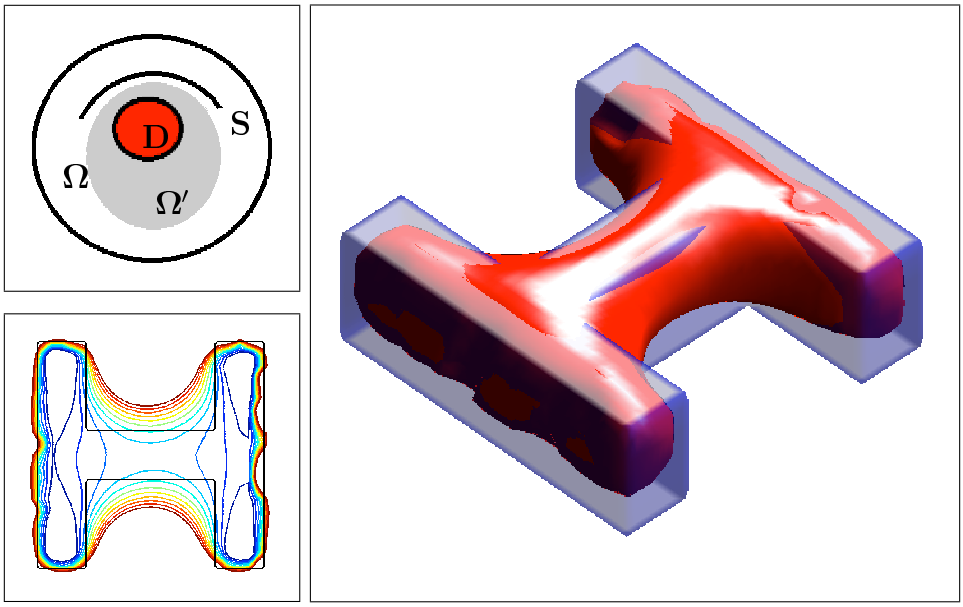

FIGURE 1. Top-left: Sketch of the geometry. Bottom-left: Isolines of the reconstruction c_n and the true object at the plane $\{(x, y, 0.4)\}$. Right: Isosurface of the reconstruction c_n (red) and the domain D of the scattering object (blue).

for all $v_h \in V_h$. If $g^h_{z,p} = (\nu \times G^h_{z,p}|_S) \times \nu$, then there holds

$$(g^h_{z,p}, v_j)_S = p \cdot \overline{V}^h_j(z).$$

Note that this identity does not hold in general, if $g^h_{z,p}$ is defined differently, e.g., by L^2-projection of $g_{z,p}$ onto the finite element (trace) space.

6. Conclusion

In this manuscript, we have proposed an alternative formulation of linear sampling methods, that does not require the explicit knowledge of a Green's function or a fundamental solution for the underlying problem. The resulting algorithms allow to sample for all test points z in the domain and several dipole directions p simultaneously. The solutions of the adjoint problems, that are required for the implementation, are also used in the evaluation of forward operators and back-projection algorithms. Therefore, the adjoint sampling methods can be integrated easily within existing code for nonlinear inverse problems. Let us finally remark that the adjoint approach is not restricted to the electromagnetic model problems discussed in this paper, but can easily be generalized to a wide range of problems, e.g., in acoustic scattering, or electrical impedance tomography. Moreover, similar techniques can also be utilized for the implementation of other sampling and probe methods.

References

[1] C. Baum. *Detection and Identification of Visually Obscured Targets* Taylor and Francis, Philadelphia, 1999.

[2] F. Cakoni, M'B. Fares, and H. Haddar. Analysis of two linear sampling methods applied to electromagnetic imaging of buried objects. *Inverse Problems*, 22:845–867, 2006.

[3] F. Collino, M'B. Fares, and H. Haddar. Numerical and analytical studies of the linear sampling method in electromagnetic inverse scattering problems. *Inverse Problems*, 19:1279–1298, 2003.

[4] D. Colton and H. Haddar. An application of the reciprocity gap functional to inverse scattering theory. *Inverse Problems*, 21:383–398, 2005.

[5] D. Colton and A. Kirsch. A simple method for solving inverse scattering problems in the resonance region. *Inverse Problems*, 12:383–393, 1996.

[6] D. Colton and R. Kress. *Inverse Acoustic and Electromagnetic Scattering Theory*. Springer, Berlin, Heidelberg, 2nd edition, 1998.

[7] D. Colton and R. Kress. Using fundamental solutions in inverse scattering. *Inverse Problems*, 22:R49–R66, 2006.

[8] R. Dautray and J.-L. Lions. *Mathematical analysis and Numerical Methods for Science and Technology. vol 3*, Springer, Berlin, Heidelberg, 1990.

[9] A. J. Devanay. Super-resolution processing of multi-static data using time reversal and MUSIC. Preprint, 2000.

[10] B. Gebauer. The factorization method for real elliptic problems. *Z. Anal. Anwend.*, 25:81–102, 2006.

[11] B. Gebauer. Gebietserkennung mit der Faktorisierungsmethode. *Dissertation*, Universität Mainz, 2006. `http://nbn-resolving.de/urn/resolver.pl?urn=urn:nbn:de:hebis:77-11370`

[12] B. Gebauer, M. Hanke, A. Kirsch, W. Muniz, and C. Schneider. A sampling method for detecting buried objects using electromagnetic scattering. *Inverse Problems*, 21:2035–2050, 2005.

[13] B. Gebauer, M. Hanke, and C. Schneider. Sampling methods for low-frequency electromagnetic imaging. *Inverse Problems*, 24:015007, 2008.

[14] M. Hanke and A. Kirsch. Sampling methods. Manuscript, 2009.

[15] B. Kaltenbacher, A. Neubauer, and O. Scherzer. Iterative Regularization Methods for Nonlinear Ill-Posed Problems. Radon Series on Computational and Applied Mathematics, de Gruyter, Berlin, 2008.

[16] A. Kirsch. The MUSIC algorithm and the factorization method in inverse scattering theory for inhomogeneous media. *Inverse Problems*, 18:1025–1040, 2002.

[17] A. Kirsch. The factorization method for Maxwell's equations. *Inverse Problems*, 15:961–75, 2004.

[18] A. Kirsch and N. Grinberg. *The Factorization Method for Inverse Problems*. Oxford University Press, Oxford, 2008.

[19] P. Monk. *Finite Element Methods for Maxwell's Equations*. Clarendon Press, Oxford, 2003.

[20] J. C. Nédélec. Mixed finite elements in $\mathbb{R}^3$. *Numerische Mathematik*, 35(35):315–341, 1980.

[21] J. C. Nédélec. A new family of mixed finite elements in $\mathbb{R}^3$. *Numerische Mathematik*, 50(35):57–81, 1986.

[22] R. Potthast. Sampling and probe methods. *Computing*, 75:215–235, 2005.

[23] J. Schöberl. NETGEN – An advancing front 2d/3d-mesh generator based on abstract rules. *Comput. Visual. Sci.*, 1:41–52, 1997.

[24] J. Schöberl and S. Zaglmayr. High order Nédélec elements with local complete sequence properties. *International Journal for Computation and Mathematics in Electrical and Electronic Engineering (COMPEL)*, 24:374–384, 2005.

[25] O. Schenk and K. Gärtner. Solving unsymmetric sparse systems of linear equations with PARDISO. *Future Gener. Comp. Sy.*, 20(3):475–487, 2004.

Erschienene Preprints ab Nummer 2008/1

2008/1	P. Urthaler: Schnelle Auswertung von Volumenpotentialen in der Randelementmethode.
2008/2	O. Steinbach (ed.): Workshop on Numerical Simulation of the Maxwell Equations. Book of Abstracts.
2008/3	G. Of, O. Steinbach, P. Urthaler: Fast Evaluation of Newton Potentials in the Boundary Element Method.
2008/4	U. Langer, O. Steinbach, W. L. Wendland (eds.): 6th Workshop on Fast Boundary Element Methods in Industrial Applications, Book of Abstracts.
2008/5	D. Brunner, G. Of, M. Junge, O. Steinbach, L. Gaul: A Fast BE-FE Coupling Scheme for Partly Immersed Bodies
2009/1	G. Of, T. X. Phan, O. Steinbach: An energy space finite element approach for elliptic Dirichlet boundary control problems.
2009/2	G. Of, T. X. Phan, O. Steinbach: Boundary element methods for Dirichlet boundary control problems.
2009/3	G. Of, O. Steinbach: The All-Floating Boundary Element Tearing and Interconnecting Method.
2009/4	O. Steinbach: A note on the stable coupling of finite and boundary elements.
2009/5	O. Steinbach, M. Windisch: Stable boundary element domain decomposition methods for the Helmholtz equation.
2009/6	G. Of, W. L. Wendland, N. Zorii: On the Numerical Solution of Minimal Energy Problems.
2009/7	U. Langer, O. Steinbach, W. L. Wendland (eds.): 7th Workshop on Fast Boundary Element Methods in Industrial Applications, Book of Abstracts.
2009/8	H. Egger, M. Freiberger, M. Schlottbom: Analysis of Forward and Inverse Models in Fluorescence Optical Tomography.
2009/9	O. Steinbach, M. Windisch: Robust boundary element domain decomposition solvers in acoustics.
2009/10	M. Freiberger, H. Egger, H. Scharfetter: Nonlinear inversion in fluorescence optical tomography.